Proc. Indian Acad. Sci. (Chem. Sci.), Vol. 107, No. 5, October 1995, pp. 581–591.

Electrodeposition and dissolution of Sn–Zn alloy films on glassy carbon

V S VASANTHA, MALATHY PUSHPAVANAM and
V S MURALIDHARAN*

Central Electrochemical Research Institute, Karaikudi 623 006, India

MS received 8 December 1994; revised 12 July 1995

Abstract. Cyclic voltammetric studies were carried in mixtures of $SnSO_4$ and $ZnSO_4$ containing sodium gluconate in the *p*H range 6 to 8 at 30° and 60°C. The stannous gluconate ions hinder the deposition of zinc while zinc gluconate ions favour the tin deposition in Sn–Zn alloy formation. This formation of Sn–Zn alloy film is a regular type of alloy deposition. Stripping voltammetric curves revealed the likely presence of zinc-rich tin intermediate phases in the Sn–Zn alloy films.

Keywords. Electrodeposition; dissolution; alloy films; glassy carbon; tin–zinc alloy.

1. Introduction

The electrodissolution of binary alloy films formed electrochemically on inert substrates has been the subject of numerous investigations in recent years. The anodic dissolution studies carried on the Cu–Au alloys and Cu–30% Zn alloys revealed that the dissolution was selective for the less noble metal (Pickering and Byrne 1971; Holliday and Pickering 1973). However, the mode of dissolution varied with the mechanism of dissolution (Cheshuri and Krutikov 1988). In the galvanostatic mode the dissolution gradually changed from preferential to simultaneous, while simultaneous dissolution occurred in the potentiodynamic method. Linear sweep voltammetric studies reveal whether the alloy film exhibits an ideal solid solution [Cu–Ni], intermediate phase or intermetallic compound [Cu–Zn], simultaneous dissolution was found. Only for the eutectic type of alloys like Cu–Pb and Cd–Zn, the dissolution was selective (Carlos and Alkaine 1988; Jović *et al* 1988). On the other hand, it was considered that the dissolution was always preferential for the less noble metal (Swathirajan 1986). The Sn–Zn alloy which exhibits a simple eutectic type is chosen for our study to determine whether dissolution is selective for less noble metals or not. The type of alloy deposition and morphology of the deposit under cyclic polarisation conditions in gluconate solutions at 30° and 60°C are presented in this paper.

2. Experimental

Triangular potential sweep (CV) voltammetric experiments were carried out in Bio-Analytical Systems 100 A, USA using a conventional three-electrode cell assembly of

*For correspondence

glassy carbon (0·2 cm^2) as working electrode, platinum as counter and saturated calomel electrode as reference electrodes. The solutions under study were deoxygenated for one hour using purified hydrogen. The temperature of the cell was kept at 30° and 60°C [± 0·01°C]. Solutions were made from Analar chemicals. $SnSO_4$ solutions [$1{\cdot}5 \times 10^{-1}$ to $2{\cdot}5 \times 10^{-1}$ M], $ZnSO_4$ solutions [$1{\cdot}5 \times 10^{-1}$ to $2{\cdot}5 \times 10^{-1}$ M] and various combinations of $SnSO_4/ZnSO_4$ solutions containing 0·9 M sodium gluconate were used. In all these solutions the total metal ion to gluconate ion concentration ratio was 1:3. The *p*H of the solution was measured using a digital *p*H meter (± 0·01 accuracy).

3. Results

3.1 *$SnSO_4$ solutions*

Figure 1 presents the cyclic voltammetry in $1{\cdot}5 \times 10^{-1}$ M sodium gluconate solutions. When polarised from − 500 to − 1700 mV, the forward scan exhibited a cathodic peak at − 1200 mV. The reverse scan intersected the forward scan and the intersection potential was found to vary with sweep rate and *p*H. However gluconate ion concentration had no effect on the intersection potential. This suggests that the deposition reaction was under diffusion control (Fletcher 1983; Fletcher *et al* 1983).

The cathodic peak potential varied with log v (120 mV decade^{-1}) and with *p*H, a value of 30 mV/*p*H was observed. The cathodic peak currents were invariant with *p*H and gluconate concentrations did not vary the cathodic peak currents and peak potentials at all sweep rates.

Increase of temperature to 60°C changed the electrochemical spectrum. The forward scan exhibited a plateau followed by a shoulder and a peak at − 1130 mV.

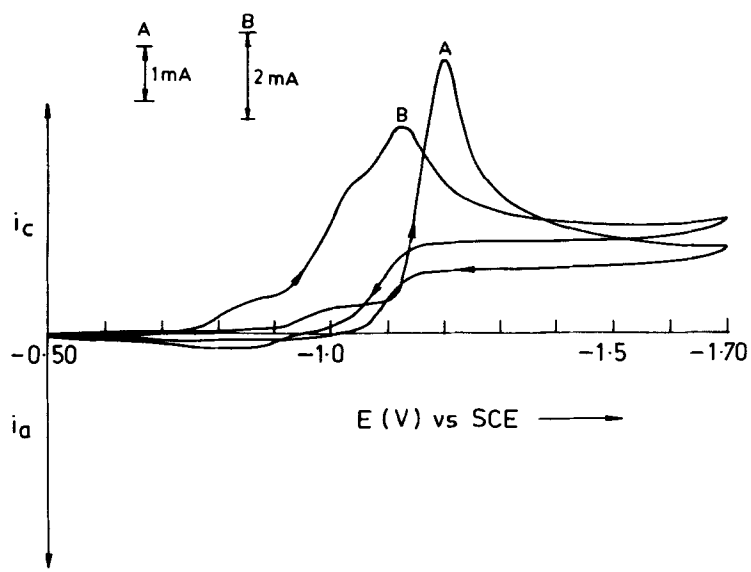

Figure 1. Typical cyclic voltammogram in 0·15 M $SnSO_4$ + 0·45 M $NaGH_4$ at *p*H 7, (A) 30°C, (B) 60°C. $E_{\lambda,a} = -500$ mV; $E_{\lambda,c} = -1700$ mV; $v = 20$ mVs^{-1}.

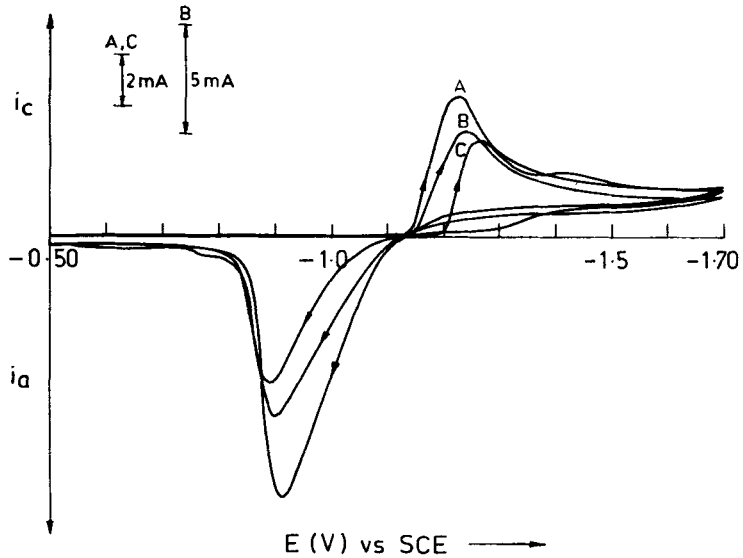

Figure 2. Typical cyclic voltammogram in 0·15 M $ZnSO_4$ + 0·45 M $NaGH_4$ solutions at different values of pH = 6 (A), 7 (B), and 8 (C). $E_{\lambda,a} = -500$ mV; $E_{\lambda,c} = -1700$ mV; $v = 20$ mVs^{-1}.

The reverse scan did not intersect the forward scan. The zero current crossing potential (ZCCP) was found to be −950 mV followed by a broad anodic peak around −875 mV. When the cathodic terminating potential was extended to −2100 mV (not shown in figure 1), hydrogen evolution started at −1800 mV. On the reverse scan, an anodic peak appeared at −1044 mV with a charge of 3·47 mC. At 60°C, the anodic peak shifted to −1029 mV though the charge that flowed under its peak increased to 5·95 mC.

3.2 *$ZnSO_4$ solutions*

Figure 2 presents the cyclic voltammogram obtained in $1{\cdot}5 \times 10^{-1}$ M $ZnSO_4$ + $4{\cdot}5 \times 10^{-1}$ M sodium gluconate solutions with a *p*H of 7.

The cathodic peak appeared at −1246 mV in the forward scan while the reverse scan exhibited an anodic peak at −900 mV. At 60°C, the charges that flowed under the cathodic peak remained the same while those of the anodic peaks increased suggesting that dissolution was favoured at 60°C. When the cathodic terminating potential was extended to −2100 mV, the hydrogen evolution reaction commenced at −1700 mV and the anodic peak potential was shifted to −810 mV. The anodic and cathodic peak potentials varied with *p*H (15 ± 5 mV/*p*H) changes at 30° and 60°C. The cathodic peak currents were nearly invariant with *p*H at 30° and 60°C suggesting that the OH^- ions did not participate in the zinc gluconate complex and its reduction to zinc.

3.3 *$SnSO_4$ + $ZnSO_4$ solutions*

Figure 3 presents the cyclic voltammogram in $SnSO_4$ + $ZnSO_4$ solutions [Sn:Zn = 1:0·5]. When polarised from −500 mV, a shoulder around −1000 mV (I) and at −1450 mV (II) a peak appeared during the forward scan. The reverse scan exhibited

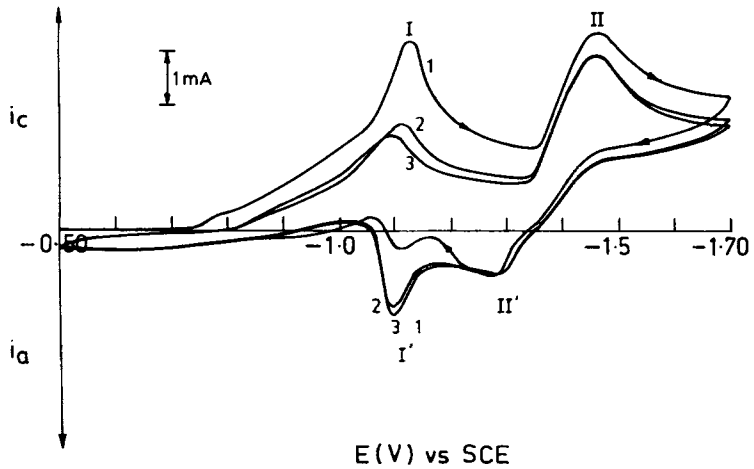

Figure 3. Typical cyclic voltammogram in 0·2 M $SnSO_4$ + 0·1 M $ZnSO_4$ + 0·9 M $NaGH_4$ solution at $pH = 7$; and 30°C – effect of scan number (1, 2, 3 scan numbers). $E_{\lambda,a} = -500$ mV; $E_{\lambda,c} = -1700$ mV; $v = 20\,\text{mVs}^{-1}$.

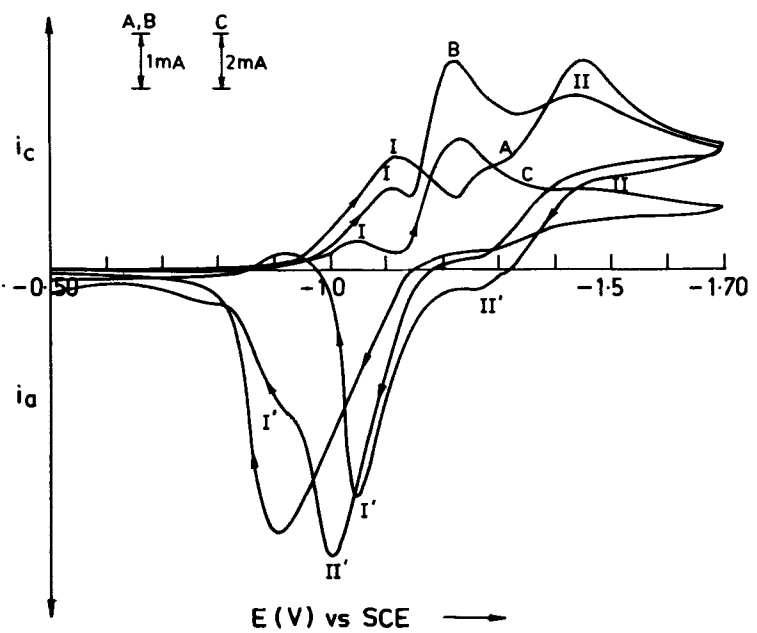

Figure 4. Typical cyclic voltammogram in 0·9 M $NaGH_4$ ($pH = 7$) containing different amounts of $ZnSO_4$ and $SnSO_4$ at 30°C. (A) 0·15 M $SnSO_4$ + 0·15 M $ZnSO_4$; (B) 0·10 M $SnSO_4$ + 0·2 M $ZnSO_4$; (C) 0·05 M $SnSO_4$ + 0·25 M $ZnSO_4$.

peaks at -1280 mV (II″) and at -1100 mV (I′). On subsequent cycling the charges flowing under peaks (I) and (II) decreased, while those under peak (II′) remained the same. The charges flowing under peak I′ increased on cycling. This suggests that on cycling, the deposition of both tin and zinc was hindered and the dissolution of tin was

favoured. The anodic and cathodic peak potentials for the dissolution and deposition of tin coincided while those for zinc differed by 170 mV. This suggests that the deposition/dissolution of tin is nearly reversible.

When the ratio of Sn:Zn in solutions was varied, the electrochemical spectrum was modified. In 1:1 solutions, the forward scan exhibited a peak at -1122 mV (I) and a shoulder around -1250 mV followed by a broad peak at -1452 mV (II) [figure 4]. The reverse scan exhibited a shoulder around -1300 mV (II) followed by a sharp peak at -1042 mV (I'). For Sn:Zn ratio (1:2) in solution, the cathodic peak (I) occurred earlier at -1110 mV, the shoulder became a new peak at -1222 mV, the peak (II') was shifted to -998 mV and the peak (I') to -900 mV. When the zinc content in the solution was increased (Sn:Zn = 1:5), the cathodic peak (I) occurred earlier and peak (II) was diminished. The new cathodic peak which appeared at -1234 mV became predominant. With increase in zinc concentration, the concentration of free zinc increased in solution and the amount of complexed zinc decreased. This caused the appearance of a new cathodic peak and the disappearance of peak (II).

4. Discussions

Gluconic acid is represented by HGH_4 where the first H refers to the carboxylic acid hydrogen and H_4 refers to the four hydrogens on the secondary alcohols (Pecsok and Juvet 1955). The anion of the gluconic acid is represented by GH_4^-. In neutral *p*H, some of the gluconate may be converted to δ-lactone and τ-lactone and it was reported that the equilibrium is

$$\left\{\frac{(H^+)(GH_4^-)}{(HGH_4)+(L)}\right\} = (1{\cdot}76 + 0{\cdot}05) \times 10^{-4},$$

and 13% of the gluconate is converted to lactones and the release of $[GH_4^-]$ is restricted by the pk_a values of the acid.

4.1 *Electrodeposition of tin*

Recently the dissociation constants of gluconic acid and the stability constants of the divalent and tetravalent tin gluconate complexes were determined (Makin and Zmbova 1991) and the divalent tin complex was found to be $Sn(GH_4)^+$ (Vasantha and Muralidharan 1994).

In order to prevent the precipitation of $Sn(OH)_2$ and to obtain a clear solution Sn: gluconate ion concentration ratios of 1:3 were used. This excess gluconate caused the invariance of cathodic peak currents and potentials on gluconate concentrations.

One may assume the reduction to take place as below

$$Sn(GH_4)^+ + e \rightarrow Sn(GH_4)_{ads},$$

$$Sn(GH_4)_{ads} + e \rightleftharpoons Sn + GH_4^-.$$

In the solution there exists a dynamic equilibrium between $Sn(OH)_2$ and $Sn(GH_4)^+$ and this was seen by the dependence of $E_{p,c}$ on *p*H.

4.2 *Electrodeposition of zinc*

Detailed voltammetric studies on the deposition of zinc gluconate complexes in the *p*H range 3·5 to 5 revealed (Vasantha and Muralidharan 1994) that the deposition of zinc is

as follows

$$Zn(GH_4)^+ + e \rightleftharpoons Zn(GH_4),$$

$$Zn(GH_4) + e \rightarrow Zn + GH_4^-.$$

As the $E_{p,a}$'s were nearly invariant with *p*H in the range of 6 to 8, the independence of $i_{p,c}$ w.r.t. *p*H suggests that the species that undergoes reduction in $ZnSO_4$ solution containing sodium gluconate is $Zn(GH_4)^+$ in this *p*H range also.

4.3 *Electrodeposition of Sn–Zn alloy films*

In $SnSO_4 + ZnSO_4$ solutions containing gluconate, the observed cathodic peak around -1100 mV (I) and -1450 mV (II) (figure 3) may be due to the successive reduction of tin and zinc in the solutions. The deposition potentials and dissolution of tin occurred at -1100 mV while those of zinc differed by 170 mV.

With increase in zinc content (figure 4), the uncomplexed zinc underwent reduction earlier to complexed zinc and when the Sn:Zn ratio was 1:5, the free zinc ion reduction was predominant and the deposition from uncomplexed zinc was favoured as shown by the shift of $E_{p,c}$ towards nobler values. The cathodic charges flowing under peaks I and II before hydrogen evolution (up to -1700 mV) were calculated.

In order to identify the type of alloy deposition (Brenner 1963) the ratio of cathodic charges of Sn:Zn to ratio of Sn:Zn in solution was calculated (table 1). It is seen that the alloy deposition follows the regular alloy deposition type up to 1:1 ratio in solution, and beyond 1:2 ratio in solutions, the less noble component in the deposit is in excess, suggesting deviation from the regular type.

4.4 *Current potential curves for tin and zinc deposition*

Figures 5 and 6 present the polarisation curves for the deposition of tin and zinc at 30° and 60°C. In presence of zinc, the deposition of tin is enhanced or the depolarisation of

Table 1. Parameters derived from cyclic voltammograms $E_{\lambda,a} = -500$ mV; $E_{\lambda,c} = -1700$ mV; $v = 20$ mVS^{-1}.

Solution composition	Sn:Zn ratio	Q_c for Sn (mC)		Q_c for Zn (mC)		Q_c ratio (Sn:Zn)	
		30°C	60°C	30°C	60°C	30°C	60°C
0·15 M $SnSO_4$ + 0·45 M $NaGH_4$	—	27·76	22·1	—	—	—	—
0·15 M $ZnSO_4$ + 0·45 M $NaGH_4$	—	—	—	32·04	32·04	—	—
0·25 M $SnSO_4$ + 0·05 M $ZnSO_4$ + 0·9 M $NaGH_4$	1:0·2	20·8	38·45	5·6	10·4	1:0·26	1:0·27
0·2 M $SnSO_4$ + 0·10 M $ZnSO_4$ + 0·9 M $NaGH_4$	1:0·5	19·84	26·4	13·44	29·6	1:0·67	1:1·12
0·15 M $SnSO_4$ + 0·15 M $ZnSO_4$ + 0·9 M $NaGH_4$	1:1	14·56	20·66	18·56	23·28	1:1·2	1:1·11
0·1 M $SnSO_4$ + 0·2 M $ZnSO_4$ + 0·9 M $NaGH_4$	1:2	10	11·2	24	49·6	1:2·4	1:4·4
0·05 M $SnSO_4$ + 0·25 M $ZnSO_4$ + 0·9 M $NaGH_4$	1:5	3·5	5·5	30·1	53·2	1:8·7	1:9·67

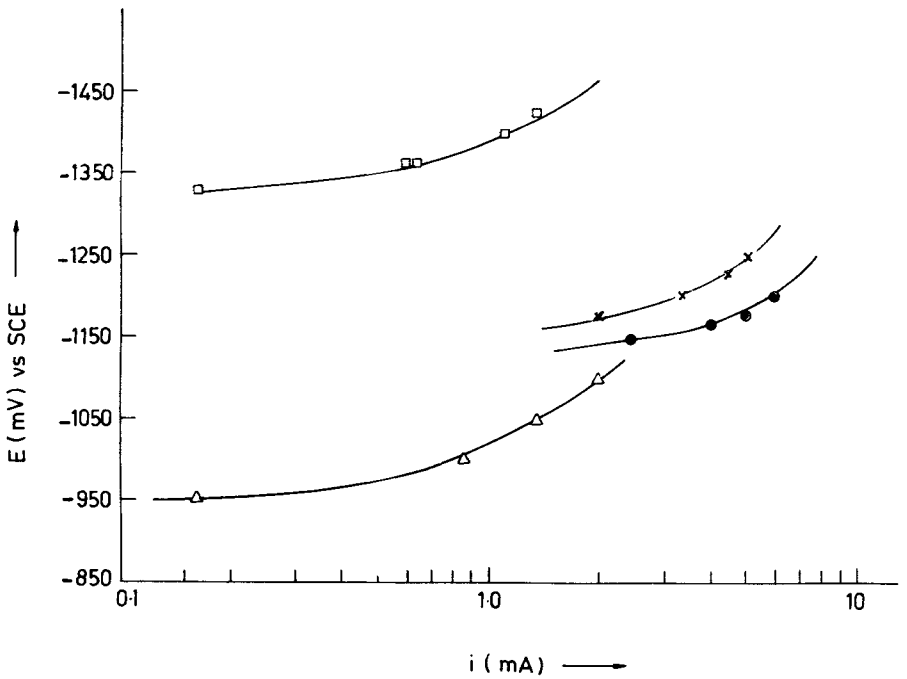

Figure 5. Potential–partial current curves for the deposition of tin, zinc and in presence of both the ions at 30°C (pH = 7). ● tin deposition from 0·15 M $SnSO_4$ + 0·45 M $NaGH_4$; × zinc deposition from 0·15 M $ZnSO_4$ + 0·45 M $NaGH_4$; Δ tin deposition from 0·15 M $ZnSO_4$ + 0·15 M $SnSO_4$ + 0·9 M $NaGH_4$; □ zinc deposition from 0·15 M $ZnSO_4$ + 0·15 M $SnSO_4$ + 0·9 M $NaGH_4$.

tin deposition occurs. Tin inhibits the zinc deposition as revealed by the enormous shift in the potentials. The inhibition of zinc deposition may be due to the submonolayer of tin deposited on glassy carbon (under potential deposition) which may inhibit the formation of clusters or nuclei of zinc.

4.5 *Dissolution of Sn–Zn alloy films*

When the cathodic terminating potentials were extended to −2100 mV, the anodic dissolution charges for zinc increased while tin dissolution was also observed (table 2) up to the Sn:Zn ratio of 1:1 in solution.

At −1700 mV, the entire surface of the electrode was covered by the Sn:Zn alloy and on the reverse scan the occurrence of potential at zero current (ZCCP) is due to the corrosion of the alloy deposit in the medium. The ZCCP's are an indication of the susceptibility of the alloy deposit to corrosion in the medium.

With increase in zinc content, the ZCCP became more active at 30° and 60°C suggesting that the dissolution is selective for the less noble metal (zinc) (table 3). The anodic peak intersection potentials became active with increase in zinc content in the deposit. Sn and Zn are soluble only in the fluid state in all proportions (Porter and Easterling 1980) and the system is the simple eutectic type. If the interaction between Sn–Zn in the solid phase is negligible, the free energy of each component in the alloy should be the same as the reversible potential of the pure component of the corresponding grain size. Thus the

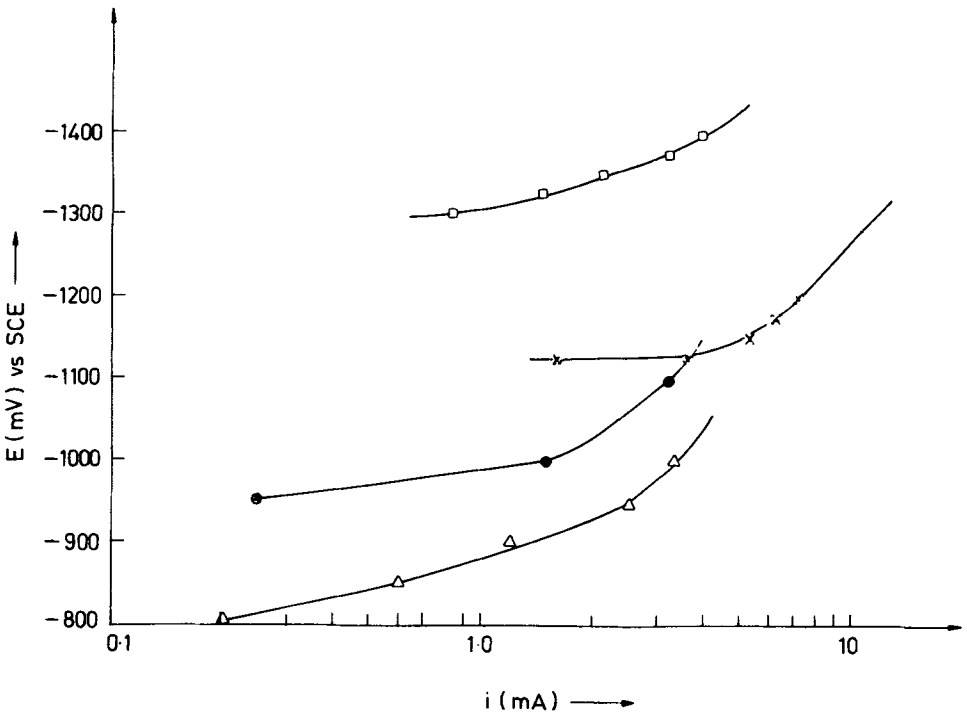

Figure 6. Potential–partial current curves for the deposition of tin, zinc and in presence of both the ions at 60°C ($pH = 7$). ● tin deposition from 0·15 M $SnSO_4$ + 0·45 M $NaGH_4$; × zinc deposition from 0·15 M $ZnSO_4$ + 0·45 M $NaGH_4$; Δ tin deposition from 0·15 M $ZnSO_4$ + 0·15 M $SnSO_4$ + 0·9 M $NaGH_4$; □ zinc deposition from 0·15 M $ZnSO_4$ + 0·15 M $SnSO_4$ + 0·9 M $NaGH_4$.

Table 2. Influence of cathodic terminating potential on anodic charges (mC) of zinc and tin dissolution at 30°C ($pH = 7$).

System	$E_{\lambda,c} = -1700$ mV Zinc	$E_{\lambda,c} = -2100$ mV Zinc	Tin
0·15 M $SnSO_4$ + 0·45 M $NaGH_4$	—	—	3·67
0·15 M $ZnSO_4$ + 0·45 M $NaGH_4$	52·1	47·62	—
0·05 M $ZnSO_4$ + 0·25 M $SnSO_4$ + 0·9 M $NaGH_4$	8·64	12·6	15·6
0·1 M $ZnSO_4$ + 0·2 M $SnSO_4$ + 0·9 M $NaGH_4$	18·56	48·1	—
0·15 M $ZnSO_4$ + 0·15 M $SnSO_4$ + 0·9 M $NaGH_4$	18·56	36·8	—

anodic branch should possess two separate dissolution peaks for each component. Below the Sn:Zn ratio of 1:1 in solution, the anodic scan exhibited two distinct peaks. However the cathodic peak intersection potentials differed very much from anodic intersection potentials for both Zn and Sn. Hence a simple case of eutectic type of alloy formation may not be present in the deposit. As the concentration of Sn:Zn ratio is increased in solution from 1:1, the dissolution peaks merged into a single peak.

Table 3. Parameters obtained from the cyclic voltammogram at 30° and 60°C (−1700 to −500 mV).

Solution composition	ZCCP (mV)		Zn dissolution intersection potential mV		Amount of Zn dissolved (μg)		ΔG (kcal/mol)
	30°C	60°C	30°C	60°C	30°C	60°C	
0·15 M $ZnSO_4$ + 0·45 M $NaGH_4$	−1146	−1146	−1148	−1100	17·6	20·08	
0·05 M $SnSO_4$ + 0·25 M $ZnSO_4$ + 0·9 M $NaGH_4$	−1154	—	−1154	—	2·92	—	−0·41
0·1 M $SnSO_4$ + 0·2 M $ZnSO_4$ + 0·9 M $NaGH_4$	−1210	—	−1240	—	6·27	—	−4·32
0·15 M $SnSO_4$ + 0·15 M $ZnSO_4$ + 0·9 M $NaGH_4$	−1315	—	−1315	−1100	6·27	14·07	−7·77
0·2 M $SnSO_4$ + 0·1 M $ZnSO_4$ + 0·9 M $NaGH_4$	−1346	−1175	−1330	−1120	—	—	−8·45
0·25 M $SnSO_4$ + 0·05 M $ZnSO_4$ + 0·9 M $NaGH_4$	−1354	−1300	−1354	−1124	—	—	−9·56

As in electrodeposited metals, the alloys are obtained at low temperature unlike in cast or thermal alloys. In order to predict the results to be obtained by electrodepositing an alloy, the phase diagram of the system should be examined in the low temperature region. However, predictions cannot be made with certainty since electrodeposits are often fine grained and fine crystal size may promote greater solubilities than estimated by a phase diagram. Therefore deviations from such diagrams may be expected. A eutectic structure may not be obtained electrically because it is formed from a melt and no parallel to such a freezing process takes place during electrodeposition.

In the case of eutectic type alloy dissolution, one would observe sharp peaks which may be ascribed to the dissolution of Sn and Zn. But the appearance of broad peaks and a single peak at higher zinc concentrations suggests that possible passivation of deposited metals may occur. Even solid-solution type of alloys exhibit (Swathirajan 1986) two separate peaks, the first peak corresponding to the preferential dissolution of the less noble metal. Jović *et al* (1988) observed a single anodic peak for the dissolution of Cu–Ni which forms a solid solution.

The appearance of single anodic peak from solutions having Sn:Zn larger than 1:1 does not present a clear picture as to whether zinc forms solid solution with tin or not. The E–i curves for zinc (figure 7) suggest that both at 30° and 60°C, the presence of tin enhanced the dissolution of the less noble metal zinc. As the amount of zinc increased in the deposit, the dissolution charge (total amount of metal dissolved) increased which may be due to the dissolution of zinc from an intermediate phase rich in zinc. The free energy change that may accompany Zn in the formation of intermediate phases may be calculated.

ΔE, the difference in the anodic peak intersection potential for both zinc and Zn/Sn alloy as a first approximation was used to calculate the free energy of alloy formation, $-2F\Delta E = \Delta G_{\text{alloy}}$ = free energy of formation of the intermediate phase.

In the formation of intermetallic compounds, one would expect that small changes in composition can cause a rapid rise in free energy change while a continuous change in

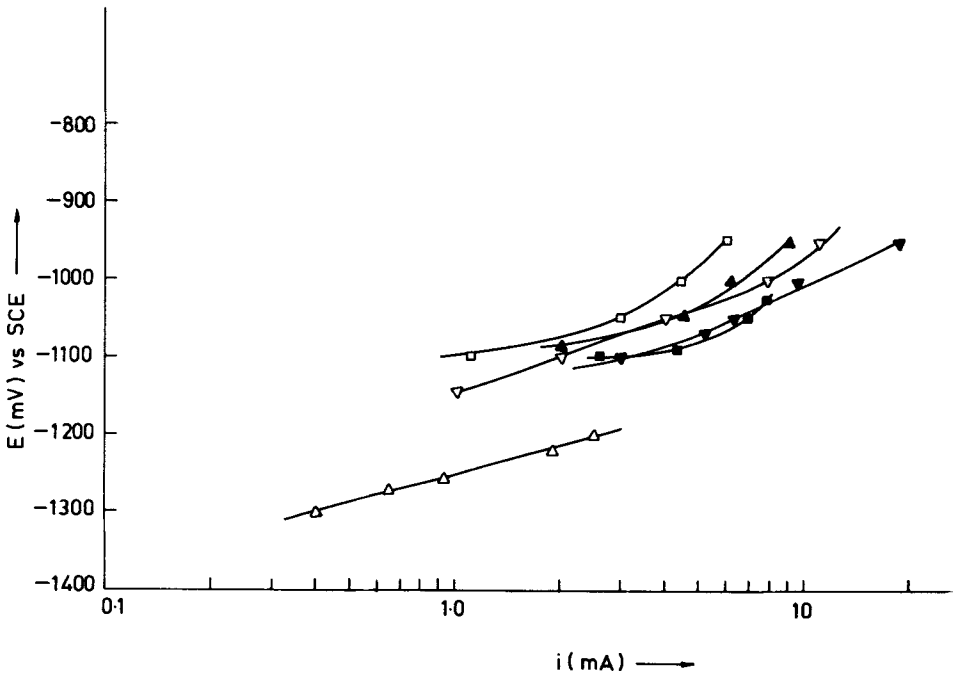

Figure 7. Potential – dissolution current curves for zinc at 30° and 60°C (*p*H 7) Δ 0·15 M $SnSO_4$ + 0·15 M $ZnSO_4$ + 0·9 M $NaGH_4$ at 30°C; ▲ 0·15 M $SnSO_4$ + 0·15 M $ZnSO_4$ + 0·9 M $NaGH_4$ at 60°C; ▽ 0·1 M $SnSO_4$ + 0·2 M $ZnSO_4$ + 0·9 M $NaGH_4$ at 30°C; ▼ 0·1 M $SnSO_4$ + 0·2 M $ZnSO_4$ + 0·9 M $NaGH_4$ at 60°C; □ 0·05 M $SnSO_4$ + 0·25 M $ZnSO_4$ + 0·9 M $NaGH_4$ at 30°C; ■ 0·05 M $SnSO_4$ + 0·25 M $ZnSO_4$ + 0·9 M $NaGH_4$ at 60°C.

free energy with composition was expected in the case of intermetallic phase formation (Porter and Easterling 1980). Table 3 presents the changes in ΔG with composition of zinc in solution. As the changes in ΔG are gradual, the formation of intermediate phase rich in zinc is visualised.

5. Conclusions

Polarisation curves for tin and zinc deposition revealed that the presence of zinc ion catalyses the deposition of tin while zinc deposition was hindered by stannous ions in the formation of Sn–Zn alloy films from gluconate solutions. The formation of Sn–Zn alloy films is the regular type of alloy deposition. Increase of zinc content in the film enhances the dissolution. Stripping voltammetric curves revealed that the film is not a simple eutectic type but also suggested the presence of zinc-rich intermediate phase formation in the alloy film.

Acknowledgement

One of the authors (VSV) thanks the Council of Scientific and Industrial Research, New Delhi for a fellowship.

References

Brenner A 1963 Electrodeposition of alloys (London: Academic Press) vol. 1, p. 76
Carlos I A and Alkaine C V D 1988 *Proceedings of Brazillian Symposium on Electrochemistry and Electroanalytical Chemistry*, Sao Paulo, Brazil, p. 338
Cheshuri A V and Krutikov P G 1988 *Electrokhimiya* **24** 1312
Fletcher S 1983 *Electrochim. Acta* **28** 917
Fletcher S, Halliday C S, Gates D, Westco M, Lwin T and Nelson G 1983 *J. Electroanal. Chem.* **159** 267
Holliday J E and Pickering H W 1973 *J. Electrochem. Soc.* **120** 470
Jović V D, Zejilovic R M, Despic A R and Stevanović J S 1988 *J. Appl. Electrochem.* **18** 511
Makin T N and Zmbova B 1991 *J. Serb. Chem. Soc.* **56** 337; cf: 1991 *Chem. Abstr.* **115** 90935
Pecsok R L and Juvet S Jr 1955 *J. Am. Chem. Soc.* **77** 202
Pickering W H and Byrne P J 1971 *J. Electrochem. Soc.* **118** 209
Porter D A and Easterling K A 1980 *Phase transformations in metals and alloys* (Workingham: Van Nostrand Reinhold)
Swathirajan S J 1986 *J. Electrochem. Soc.* **133** 671
Vasantha V S and Muralidharan V S 1994a *Proc. Indian Acad. Sci. (Chem. Sci.)* **106** 825
Vasantha V S and Muralidharan V S 1994b *Port. Electrochim. Acta* **12** 105